A multi-analytical approach for precise identification of alkyd spray paints and for a better understanding of their ageing behaviour in graffiti and urban artworks

A multi-analytical approach for precise identification of alkyd spray paints and for a better understanding of their ageing behaviour in graffiti and urban artworks

G. Pellis[1], M. Bertasa[1], C. Ricci[2], A. Scarcella[2], P. Croveri[2], T. Poli[1], D. Scalarone[1*]

[1] Department of Chemistry, University of Torino, Via Pietro Giuria 7, Torino, Italy;
giulia.pellis@unito.it, moira.bertasa@unito.it, tommaso.poli@unito.it
[2] Fondazione Centro Conservazione e Restauro "La Venaria Reale", Venaria Reale, Torino, Italy;
chiara.ricci@centrorestaurovenaria.it, arianna.scarcella@centrorestaurovenaria.it,
paola.croveri@centrorestaurovenaria.it
* Corresponding author: dominique.scalarone@unito.it

Abstract

Contemporary graffiti and murals became an artistic expression worthy of attention worldwide as well as their conservation. The application of spray paints with increasing technical performance mirrors the variety of the chemical composition of these increasingly common painting materials. An insight into the formulation and the ageing process is extremely important to predict and prevent the possible decay phenomena observed on outdoor urban artworks.

This paper aims to investigate the relationship between the macroscopic outcomes and the chemical changes occurring on spray paints after the ageing by a multi-analytical approach. A systematic artificial ageing procedure was performed on multiple sets of concrete mock-ups painted with three different alkyd-based spray paints and in three different light-sensitive colours. The colour variation was assessed by colorimetric measurements, the changes in the paint cross section were observed by scanning electron microscopy, Fourier transform infrared spectroscopy (FTIR) was applied both to characterize the spray paints and to detect the chemical changes of the organic compounds during the ageing.

A significant and innovative contribution to this research is the application of the evolved gas analysis-mass spectrometry (EGA-MS) and pyrolysis-gas chromatography/mass spectrometry (Py-GC/MS) with tetramethylammonium hydroxide in double-shot mode. These two analytical methodologies allowed an accurate classification of the different alkyd-based binders, the identification of plasticizers, organic pigments and other components often hard to spot in complex formulations, and an analysis of their fate following ageing.

Keywords
Spray paint; alkyd; mural; double-shot pyrolysis-GC/MS; tetramethylammonium hydroxide; organic pigment

1. Introduction

Spray paints are a combination of paint and propellant which can be sprinkled in the form of an aerosol through a nozzle. At that stage, the propellant easily evaporates and leaves droplets of paint on the surface.

Spray paints have lots of advantages over traditional paints, such as the ability to colour and adhere to a wider variety of supports, like fabrics, plasters, glass and metals; they are extremely versatile products, providing a satisfying degree of coverage in a single application, quick drying and practical storage, thanks to the easy-to-handle packaging. These excellent properties made the fortune of these products for both industrial applications and household products.

An emerging field of interest for spray paints is the creation of contemporary graffiti and murals. In particular, murals, as well as street art works, are often used in the context of urban regeneration projects to improve the condition of urban neighbourhoods or to recall historical and significant events. However, time and atmospheric agents prevent murals from lasting along decades [1-4], to the point that their maintenance and conservation has recently become the subject of debate and concern within local communities, administrators, public and private bodies [5-9].

Usually, street artists choose paints and other graphic means based on artistic considerations, related to the painting technique or aesthetic performance, overlooking the durability; traditional paint materials are often replaced or mixed with products meant for industrial or domestic uses to enhance certain properties. Further, street artists are used to changing their own materials and application methods, actually complicating the implementation of any conservation procedure for preserving murals or restoring those that are already affected by degradation [10]. Therefore, it is important to exactly know the chemical composition of the painting materials and the degradation processes they may undergo, to develop proper conservation strategies.

The formulation of modern paints became ever more complex over the years due to the improvement of the technologies employed for their preparation and the chemical composition of the exploited components. Furthermore, the demanding requests of the growing market contributed to launch different types of spray paints. From a chemical point of view, the main components of paints are the binding medium, pigments and extenders. Paints used by most of the contemporary muralists and street artists are based on alkyd resins, acrylic resins, styrene-acrylic resins and

styrene resins. At times, minor binders are added as modifiers, such as nitrocellulose, poly(vinyl phenyl ketone) and chlorinated rubber [11-13]. Besides pigments and extenders, other additives may be used in small quantities to improve the performance of the paint in terms of shelf life, easy application, durability, health and safety requirements [14]. The multi-analytical approach has proved to be the most suitable for an accurate characterization of complex systems such as spray paints. A first complete set of compositional data was published by Germinario et al. who analysed 45 spray paints from different brands and manufacturers, of which about half were identified as alkyd-based, the other half styrene-acrylic, while only a few products were based on styrene resins [11].

On the other hand, there is still little research devoted to studying the effects of aging on the composition and properties of spray paints. Spray paints, as paints in general, undergo different ageing reactions. Each component can strongly affect the overall photo-stability of the paint. One of the most severe causes of degradation is solar radiation. Solar light triggers photo-degradation reactions which generate radical fragments readily reacting with oxygen. Generally, photo-oxidation starts on the very superficial layer of the paints, moving within the layer later on [15,16]. The rate of photo-oxidation depends on several factors, like radiation, oxygen diffusion, time of exposure, and on the characteristics of the materials and the surrounding environment [17, 18]. The additives or pigments into the paint formulation may also influence the photo-oxidative reactions. For example, pigments can either promote or prevent photo-degradation reactions. Some inorganic pigments promote ageing processes [19], while others tend to improve durability in comparison to the organic counterparts [14]. Indeed, organic pigments are by their nature less stable and more light-sensitive, with some exceptions though (e.i. blue phthalocyanine pigments [15] are relatively stable).

In the past four years, over 50 murals, graffiti and urban artworks were studied as part of a research project focused on the conservation of art in public spaces. An analytical campaign was carried out on a wide range of artworks aimed at identifying the painting materials and their state of conservation.

This diagnostic campaign highlighted that alkyd and modified alkyd resins are the most prevalent binder in spray paints used in urban artworks worldwide, regardless of the type of support [20]. Alkyd resins are polyesters modified by fatty acids. Polyester prepolymers are obtained by condensation polymerization of dicarboxylic acids or anhydrides (i.e. phthalic acid or anhydride, maleic acid, etc.) and polyols (i.e. glycerol, pentaerythritol), and are reacted with unsaturated fatty acids which become part of the structure of the polyester. Once the paint is sprayed, the C=C bonds of the fatty fraction react by photo-oxidation to give a cross-linked structure and paint curing,

similar to what happens for siccative oils, but faster. Additional compounds, such as styrene and nitrocellulose, are often added in the final formulation to improve the paint performances.
The assessment of the state of conservation of the artworks pointed out major decay phenomena, such as loss of material and chromatic alterations [21]. The loss of material was frequent on any kind of substrate (i.e. plaster, bricks, concrete). Lacunas and abrasion were the most common effects, involving the paint layers, the background layer or both. In the superficial paint layers, cracking and flaking were observed as well. Fading and darkening are the main chromatic alteration modifying the appearance and perception of the artworks, especially for those more exposed to direct sunlight.
A set of mock-ups were prepared to better understand the relationship between the degradation processes of the paints and the macroscopic effects of degradation, visible to the naked eye. The mock-ups were covered by alkyd spray paint and then artificially aged. The changes in the optical properties of the paints were monitored over time by colour measurements, visible diffuse light and ultraviolet-induced visible fluorescence photography. Fourier transform infrared spectroscopy (FTIR) provided information on the organic and inorganic components of the paints and the spectral changes that occur during aging due to degradation processes. This information was complemented by scanning electron microscopy of the cross sections, to evaluate any changes in the morphology and thickness of the paint. Compositional details before and after ageing of the spray paints were obtained by evolved gas analysis-mass spectrometry (EGA-MS) and pyrolysis-gas chromatography/mass spectrometry (py-GC/MS). In particular, py-GC/MS was performed in double-shot mode, where the sample undergoes to a first heat treatment at low temperature, in conditions of hydrolysis and thermally assisted methylation induced by tetramethylammonium hydroxide (TMAH), and a subsequent pyrolysis step at high temperature, to investigate the composition of the chemically more resistant binder fraction. In general, pyrolysis without derivatization is sufficient to identify the alkyd binder and was also used successfully to identify acrylic and poly(vinyl phenyl ketone) secondary binders and additives [11]. However, derivatization with TMAH is particularly useful for characterizing the fatty acid profile of alkyd resins and other polar components, often difficult to detect as such because they are not very volatile. Combining the use of TMAH with the double-shot mode could help to improve understanding of the behaviour of alkyd spray paints over time. To the best of our knowledge, this is the first study that reports analytical pyrolysis data of alkyd resins in double shot and with derivatization with TMAH.

2. Experimental

2.1. Materials

Three types of spray paints were chosen, of different colour, brand and manufacturer, as described in Table 1.

The mock-ups were prepared with i.work TECNOCEM 32.5 R by ITALCEMENTI, a Portland concrete with limestone type II, characterized by a strong resistance in the drying phase. According to the UNI EN 197-1 standard, the product contains 80% up to 94% of clinker, while the remaining fraction consists of limestone (TOC ≤ 0.20%, in mass (LL)) and other minor constituents. The Portland concrete was added with local river sand in the ratio 1:3 and afterward mixed manually with water to facilitate the processing of the mortar.

Silicone moulds were used to shape the mock-ups (8 cm x 5.5 cm x 2 cm). They were air-dried for two months before the application of the alkyd spray paints at a distance of approximately 20-30 cm. Then the mock-ups were artificially aged by alternating cycles of exposure to artificial solar light and wet-dry cycles. Each cycle included: a) 100 hours of light ageing in a Q-Sun Xe-1 Xenon Test Chamber (Q-Lab Corporation, UK), at constant temperature of 50 °C, irradiance set at 0.68 W/m^2 at 340 nm and Daylight Q filter (cut-on at 295 nm), simulating exposure to direct sunlight, b) 50 hours in a self-made humid chamber consisting of a closed box with water on the bottom, which reaches equilibrium at 85% RH after 5 hours, and c) 50 hours in an oven at 40 °C. Overall, the ageing lasted 8 cycles for a total of 1600 hours.

2.2. Characterization

The mock-ups were characterised by colorimetric measurements, Fourier transformed infrared spectroscopy (FTIR), scanning electron microscopy (SEM), evolved gas analysis-mass spectrometry (EGA-MS) and pyrolysis-gas chromatography/mass spectroscopy (Py-GC/MS). For FTIR and thermal analyses, sampling was performed with a scalpel, paying attention to removing only the paint without removing part of the concrete substrate.

2.2.1. Colour measurements

Colour measurements were performed to assess colour stability of the paints over time. Colour data were obtained using a Portable Spectrophotometer CM-700d KONICA Minolta in SCI (specular component included) mode; a total of 15 measurements (5 sites of measure, 3 measurements for each site) were acquired for each mock-up, then the average values were calculated. The change of colour (ΔE^*_{ab}) was calculated for each area comparing colour coordinates L*, a*, b* obtained before and after the ageing. The CIELAB colour space, also referred to L*a*b*, is a three-dimensional space defined by the International Commission on Illumination (CIE) in 1976. The colour is expressed

through three values: L*, a* and b*. L* defines lightness, it goes from 0 to 100 where 0 is referred to black and 100 to white. a* is a chromatic scale that expresses the colour tendency to green (negative values) or red (positive values). Finally, b* is the chromatic scale that represents how much a colour tends to blue (negative values) or yellow (positive values). The differences between two colours are expressed through the parameter ΔE^*_{ab}. This represents the Euclidean distance between the two colours and is calculated according to the following equation:

$$\Delta E^*_{ab} = \sqrt{(\Delta a^*)^2 + (\Delta b^*)^2 + (\Delta L^*)^2}$$

The ΔE^*_{ab} error was estimated through the propagation of errors with the calculation of partial derivatives.

2.2.2 Visible diffuse light photography and ultraviolet-induced visible fluorescence photography

The photographic documentation allowed to record the surface characteristics of the samples and the colour change due to the ageing. The use of a UV source to illuminate the samples can help distinguish different materials or effects of ageing, due to the specific response of the surface to UV rays.

For visible diffuse light photography, lighting was achieved by placing 2 800W Ianiro Varibeam Halogen lamps to the right and left of the set of mock-ups, at an angle of approximately 45° to the normal to the surface, and with the aid of umbrellas. Photographs were taken with a Nikon D810 Full-Frame DSLR camera equipped with a complementary metal oxide semiconductor (CMOS) sensor, providing a resolution of 7360 x 4912 pixels.

For the ultraviolet-induced visible fluorescence (UVF) photography, the lighting was achieved by means of two Labino UV Floodlight spot lamps with emission peak at 365 nm, approximate distribution angle of 3.5°, and irradiation 4500 μW/cm^2. For the acquisition of the images the camera Nikon D810 Full-Frame DSLR was equipped with a complementary metal oxide semiconductor (CMOS) sensor and Hoya UV-IR Cut filters, providing a resolution of 7360 x 4912 pixels in the 400-780 nm spectral range.

In both cases, the image processing was carried out by means of Adobe Lightroom and Adobe Photoshop softwares, included a color correction conducted by inserting a 24-color ColorChecker Classic reference in the field of view.

2.2.3. Fourier Transform Infrared Spectroscopy (FTIR)

FTIR spectroscopy gave information on the inorganic and organic components of the spray paints. FTIR analyses were carried out with a Spectrum 100 instrument (Perkin Elmer, Weltham, MA,

USA) in attenuated total reflectance (ATR) mode with a diamond crystal, using 16 scans at 4 cm^{-1} resolution in 4000-650 cm^{-1} spectral range.

2.2.4. Evolved gas analysis-mass spectrometry (EGA-MS) and pyrolysis-gas chromatography/mass spectrometry (Py-GC/MS)

Mass spectrometric analyses provided detailed information on the composition of the major alkyd binder, on any other binders, on organic additives and pigments, and on their fate upon ageing.

For EGA-MS and Py-GC/MS analyses, samples were derivatized with the Thermally Assisted Hydrolysis and Methylation method (THM) using tetramethylammonium hydroxide (TMAH) in aqueous solution at a concentration of 25% by weight (Sigma-Aldrich, Italy). A micro-furnace Multi-Shot Pyrolyzer EGA/Py-3030D (Frontier Lab, Japan) coupled to a GC/MS system was used. Samples were placed into a stainless steel cup, added with 5 µL of TMAH solution and inserted into the micro-furnace.

For EGA-MS analyses an Ultra ALLOY hollow steel column (2.5 m, 0.15 mm i.d.) was used to connect the pyrolyzer to the mass spectrometer. The column was thermostated at 300 °C in the GC oven of a 6890N Network GC System (Agilent Technologies, USA). The initial temperature of the micro-furnace was set at 50 °C, followed by a ramp of 20 °C/min up to 730 °C. The carrier gas was helium (1.0 mL/min) and split ratio was 1/20 of the total flow. The mass spectrometer was a 5973 Network Mass Selective Detector (Agilent Technologies, USA). Mass spectra were recorded under electron impact at 70 eV, scan range 40-600 m/z. The MS transfer line was kept at 280 °C, the ion source at 230 °C and the quadrupole mass analyzer at 150 °C.

Py-GC/MS analyses were performed in double-shot mode with the same pyrolyzer and GC/MS system used for EGA-MS analyses. For the first shot the pyrolysis temperature was set at 240 °C and kept for 1 minute. In the second shot the sample was pyrolyzed at 600 °C for 12 seconds. The interface temperature of the pyrolyzer was 300 °C and the temperature of the GC injector was kept at 280 °C. The GC was equipped with a methylphenyl-polysiloxane cross-linked 5% phenyl methyl silicone (30 m, 0.25 mm i.d., 0.25 µm film thickness) capillary column. The carrier gas was helium (1.0 mL/min) and split ratio was 1/20 of the total flow. The following temperature program was used for the gas chromatographic separation: isotherm of 2 minutes at 50 °C, ramp of 10 °C/min up to 300 °C, isotherm at 300 °C for 5 minutes. Mass spectra were the same described for EGA-MS analyses. All instruments were controlled by Enhanced Chem Station (ver. 9.00.00.38) software. The mass spectra assignment was done with the Wiley 138 and NIST2008 libraries and by comparison with literature data.

2.2.5. Scanning Electron Microscopy (SEM)

SEM was used to analyse the paint cross section. Tiny fragments were sampled from the mock-ups and were embedded in a synthetic transparent epoxy resin; the face perpendicular to the paint layer was polished to obtain a flat mirror surface to be observed with a Zeiss EVO60 scanning electron microscope equipped with a lanthanum hexaboride (LaB6) cathode and a silicon drift detector (SDD). Samples were analysed without any pre-treatment in variable pressure mode, using an accelerating voltage of 20 kV and a pressure of 20 Pa at different magnifications in the range 450-1000x.

3. Results and Discussion

After 800 hours of exposure to artificial solar light and to wet-dry cycles for other 800 hours, most of the paints underwent colour changes equivalent to ΔE values between 2 and 3 (Figure 1), deeming ΔE=3 the threshold value of the colour differences objectively visible to the human eye. Actually, colour differences are easily perceived by the human eye for values of ΔE>3; for 2<ΔE<3 the colour differences are less evident and not recognised by all observers; if ΔE<1, the human eye is unable to make any distinction [22].

The variations that the CIELAB colour coordinates underwent as a result of ageing are shown in Table 2. In general, the paints with the greatest variation were the red spray paints. In particular, the red Montana94 paint showed a ΔE = 2.77, due to an increase in L* and a decrease in the a* and b* coordinates (i.e. the colour became lighter and turned into colder shades); the red Montana Gold showed a ΔE = 2.26, with a decrease of the coordinates a* and b* (i.e. the colour turned towards colder shades), while the red Belton Molotow recorded a ΔE = 3.03, due to an increase in L* and a reduction in a* and b* (i.e. the colour became lighter and turned to colder shades).

Considering that the ΔE colour change values were lower than the threshold value 3 in almost all the cases, only slight colour differences were observed through the photographic documentation of the mock-ups under diffuse visible light (Figure 2, top). Whereas the images with visible fluorescence induced by UV radiation clearly highlighted some variations after ageing (Figure 2, bottom). Although an interpretation of this behaviour is complex, the visible fluorescence exhibited a significant colour variation in whole samples, partly related to the degradation of the alkyd binder. In fact, the time-limited ageing highlighted variations in the structure and composition of the alkyd binders, discussed in detail in the following paragraphs.

Prior to mass spectrometry analyses, ATR-FTIR spectra were collected to get preliminary information on the binder and inorganic components of the paints. Despite the presence of intense absorptions of the inorganic fillers, the characteristic absorption bands of the alkyd resins were well

distinguished in all the samples [23]: OH stretching (3600 - 3100 cm^{-1}), CH stretching (2957, 2855 cm^{-1}), C=O stretching (1730 cm^{-1}), COO asymmetric stretching of the ester group (ca. 1270 cm^{-1}), CCO asymmetric stretching (ca. 1070 cm^{-1}), C=C stretching of aromatic rings (1489, 1450, 1580 cm^{-1}), out-of-plane bending of aromatic CH (between 750 and 700 cm^{-1}). In the Belton Molotow and Montana Gold samples, the nitrocellulose component was clearly identified by the intense absorptions of the NO_2 stretching (1645 cm^{-1}) and C-N stretching (835 cm^{-1}), while in Montana Gold no specific signals of the acrylic component declared by the manufacturer were found. In some cases, FTIR spectra showed small peaks or shoulders, probably due to the absorption of organic pigments. However, the interference of the other paint components did not allow a precise identification of the pigments. Silicates were detected in all the paints (at approximately 1000-1015 cm^{-1}), in particular, talc in Belton Molotow paints (3675 cm^{-1}). Moreover, PW6 (titanium white) and PY42 (hydrous ferric oxide) were found in green Montana94.

In Figure 3, the spectra of the unaged and aged red paints of the three brands were compared to identify the chemical changes undergone in time. The spectra were normalized to the silicate absorption band at about 1005 cm^{-1}, not affected by ageing. For all types of alkyd sprays, a general intensity decrease of the absorption bands was observed, except for the OH stretching (between 3100 and 3600 cm^{-1}). In this range, a slight increase was observed as a result of radical oxidative processes due to the exposure to UV light or to hydrolysis reactions of alkyd-binder ester groups. In particular, for the Montana94 series of paints, a widening of the absorption band of the ester carbonyl to higher wavenumbers was recorded, compatible with the formation of oxidation products of the alkyd component, as reported in the literature [24-26]. However, the general trend observed in all the samples is a strong decrease of all the absorption bands related to the organic component. This behaviour characterizes both the signals of the alkyd binder (1725, 1276 cm^{-1}) and those of the nitrocellulose (1650, 835 cm^{-1}) if present, pointing out a thinning of the paint layer due to scission reactions with the release of volatile fragments and/or additives. Figure 4 exemplifies the thinning in the case of the black Montana94 spray paint and shows a decrease in paint thickness from about 26 μm in the unaged mock-up to 10 μm in the aged one.

Although very useful for identifying the type of binder, the presence or absence of nitrocellulose (not detectable for example by Py-GC/MS) and the type of inorganic fillers, FTIR spectra cannot provide detailed information on the composition of the major alkyd binder and any minor binders, on organic additives and pigments, and on their fate upon ageing.

These issues were addressed by EGA-MS and Py-GC/MS analyses. Figure 5 shows the EGA-MS curve of the aged and unaged Belton Molotow paints as an example. The analysis was performed by adding a few drops of TMAH to the sample. Following the thermally assisted hydrolysis and

methylation reaction, most of the organic binder turns into volatile compounds between 150 °C and 300 °C, with a maximum at 240 °C. The second zone of volatile emission, between 300 °C and 500 °C, corresponds to the degradation of the residual polymeric component of the binder, not yet volatilized by the thermochemolysis which occurs at lower temperatures.

No significant differences were observed in the EGA profiles of the aged and unaged samples. The anomalous behaviours were found once again in the reds, especially in the aged Montana Gold and Montana94 paints, where the release of volatile products occurred at lower temperatures than in the other samples. On the other hand, in the red Belton Molotow sample, the release of volatiles between 300 °C and 500 °C were relatively higher than in the other samples and a little shifted towards higher temperatures.

Following the EGA-MS analyses, the temperatures of 240 °C and 600 °C were identified as ideal temperatures to detect the products of hydrolysis and thermally assisted methylation of the paint samples, along with the pyrolysis products of the least volatile component of the samples.

A pyrolysis temperature of 240 °C was enough to induce the hydrolysis and methylation of ester groups. In fact, the first shot of the Py-GC/MS analysis resulted in a large number of fragments, identifying the main structural units of the alkyd resins and allowing their differentiation. Additives with low molecular weight and some pyrolysis markers of organic pigments were also detected in this step of the analysis. In addition, residual fragments of the alkyd resin and more thermally stable organic pigments were detected in the pyrolysis step at 600 °C.

Table 3 reports the main peaks identified in the three brands of spray paints at the pyrolysis step at 240 °C. Figure 6 shows the pyrolysis-GC/MS curves of the black paints. Chemical differences were detected in the alkyd component and in the overall formulation that only mass spectrometric techniques can recognise. First of all, the composition of the polyester component of the alkyd binders is different: in Montana94, the main components of the alkyd binder are glycerol, benzoic acid, pentaerythritol, phthalic acid, azelaic acid, palmitic acid, stearic acid, oleic acid, linoleic acid and a compound eluted at 22.5 minutes, tentatively assigned to a dihydroxy-octadecanoic acid; in Montana Gold, the alkyd fraction contains glycerol, an unknown aliphatic carboxylic acid tentatively assigned to 3,5,5-trimethylhexanoic acid, pentaerythritol, phthalic acid, a very low content of fatty acids and a significant amount of bis(2-ethylhexyl)-adipate with the function of plasticizer; Belton Molotow sprays reports hydroxy benzoic acid, an unknown aliphatic carboxylic acid, pentaerythritol, phthalic acid, palmitic acid, stearic acid, oleic acid and linoleic acid.

All the acids and alcohols just mentioned were detected in the form of methyl derivatives (i.e. methyl esters or methyl ethers) following the reaction with TMAH. An exception is the plasticizer bis(2-ethylhexyl)adipate, which is itself an ester and in the conditions of thermally assisted

methylation at 240 °C was detected as such, at about 22.9 minutes, and as 2-ethyl-hexanol and dimethyl hexanedioate, two fragments deriving from the cleavage and methylation of the two ester groups (Figure 7). It is worth to notice that dimethyl hexanedioate could also be a marker of hexandioic acid (i.e. adipic acid), that, similarly to phthalic acid, can be a dicarboxylic acid used in the synthesis of some types of alkyd resins.

The pyrolysis step at 600 °C provided some additional information useful for a correct interpretation of the pyrolysis markers and composition of the paints. In all the samples, the polyol markers disappeared or were much less intense than in the first pyrolysis step, while the synthetic mono and dicarboxylic acids and their derivatives (i.e. benzoic acid, phthalic acid and phthalic anhydride) were the most significant peaks (Table 3). In particular, the pyrograms of the Montana Gold sprays show that styrene is also present in the binder, thus suggesting that the alkyd resin was styrene-modified. Styrene is usually added to the alkyd formulation to improve the surface brilliance and mechanical resistance. On the other hand, the presence of other binders, such as acrylic copolymers, was excluded in both Montana94 and Belton Molotow, while in Montana Gold spray paint only a very little signal of methyl methacrylate was detected. Since in the conditions of analysis the acrylic binders would be difficult to identify due to the hydrolytic action of TMAH, which leads to a strong fragmentation of the acrylic units, the spray paints were analysed even without thermally assisted methylation and again traces of acrylic markers were detected only for the Montana Gold paints.

Py-GC/MS analysis also allowed to identify some markers of organic pigments, in the first or second shot depending on the thermal stability and volatility of the pigment (Table 3). Markers of red pigments were identified in the first shot: in the red Montana Gold, N-methyl-o-toluidine, 1,2,4-trichloro-benzene, 2,4,5-trichloro-benzenamine, as characteristic markers of PR112; in red Montana94 and green Montana Gold, 2-methoxy-benzenamine and N-methyl-2-methoxy-benzenamine, as markers of azo pigments of the 3-hydroxy-2-naphthalenide type (i.e. PR9, PR188). However, other markers were expected for these pigments but not detected in the sample, thus the identification remains uncertain. Lastly, 2-ethoxy-benzenamine is a marker of PR170, identified in the red Belton Molotow; also in this case, other markers expected for this pigment were absent, with a consequent uncertain identification [27,28].

Instead, markers of phthalocyanines were identified in the pyrolysis step at 600 °C. Phthalocyanines are difficult to detect because they are very stable also under pyrolysis conditions and are not volatile enough to be eluted in the gas chromatograph column. The only fragments of pyrolysis that can suggest their presence in the formulation are 1,2-benzendicarbonitrile and 4-cyano-benzoic acid

(here identified as methyl ester) [29]. Both fragments were detected in Montana94 and Montana Gold green paint, while only 4-cyano-benzoic acid was identified in the green Belton Molotow.
In general, the Py-CG/MS curves of the aged samples are very similar to the unaged ones, but a few relevant differences were detected and correlated to the ageing of the spray paints (Table 4). First of all, a relevant effect of the ageing is the decrease or disappearance of oleic and linoleic acids whose unsaturations in the position C9 and C12 were involved in the oxidative cross-linking reactions that are responsible for the drying and hardening of the paint. These changes in the structure and composition of the alkyd binder are all observed in the analyses carried out at the pyrolysis temperature of 240 °C, while the more stable fraction of the binder, that does not decompose in the first step of pyrolysis, remains substantially unchanged during ageing.
Another effect of the ageing is that the plasticizer, when present in the unaged paints, disappears or strongly decreases due to its migration from the bulk of the paint to the surface from where then it leaves the samples. Also, the peak assigned to hexanedioic acid dimethyl ester, detected in the unaged samples, disappears in the aged ones, clearly indicating that it is a pyrolysis fragment of bis(2-ethylhexyl) adipate. This allows to eliminate any ambiguity about the origin of the hexanedioic acid, which is therefore a marker of the plasticizer and not of the alkyd resin. Finally, most of the markers of organic pigments identified in the unaged samples were detected also in the aged paints, but the markers of azo pigments are in general a little less intense compared to the unaged paints, while the phthalocyanines appear more stable.
The stiffening and embrittlement of the paint film caused by the loss of plasticizers, by the oxidative ageing of the fatty acid component of the alkyd binders and by the thinning of the paint films, are reflected in the conservation problems found on contemporary outdoor murals and on street art works.
Similarly, the greater chemical stability of phthalocyanines (i.e. blue and green paints) compared to azo pigments, corresponds to the phenomenology of the chromatic alterations recorded in many real works of art.
Figure 8 shows a mural made during PicTurin – Torino Mural Art Festival, in 2012, in Turin, Italy. The mural was made with alkyd spray cans on a concrete wall. The most evident signs of degradation, apart from vandalic writings, are flacking, fractures, loss of material with formation of lacunas, and a widespread yellowing and chromatic alteration: areas these days light pink, almost white, were originally red or magenta, areas that now are yellow were orange and what originally was brown now appears green.
The Py-GC/MS of the paint sampled in a point of the mural formerly brown and currently green is shown in Figure 9. The profile of the curve is very similar to that of Montana94 paints and

corresponds to an alkyd consisting of glycerol, benzoic acid, pentaerythritol, phthalic acid, azelaic acid, palmitic acid, stearic acid, oleic acid, linoleic acid and dihydroxy-octadecanoic acid. Both pyrolysis markers of phthalocyanine blue (i.e. 1,2-benzendicarbonitrile and 4-cyano-benzoic acid) were identified, even if the intensity of the peaks was very low. In addition, PW6 and PY42 were also identified by FTIR. Therefore, the brown paint used for the mural was probably a Montana94 product containing a mixture of pigments some of which have degraded, leaving the paint a green hue resulting from a combination of yellow (i.e PY42) and blue (i.e. PB15).

4. Conclusion

Although the artificial ageing applied in this study produced milder effects than observed in many real cases, it was sufficient to identify correlations among the changes in composition, structure and properties of aged spray alkyd paints and the visible effects of the degradation processes occurring in real artworks.

The multi-analytical characterization of mock-ups reproducing murals with alkyd spray paint allowed to investigate some chemical aspects related to the degradation of contemporary wall paintings. If the colour change, measured by monitoring the coordinates L*, a* and b* during artificial ageing, appears to be mostly related to the stability of the pigments, the variations in the chemical and molecular characteristics of the binders (i.e. oxidation, loss of plasticizers, cross-linking of unsaturated fatty acids, presence or absence of property modifiers) are more associated to the changes in the adhesion and cohesion of the paints observed in real case studies.

The adopted analysis plan included colour measurements, scanning electron microscopy, infrared spectroscopy and mass spectrometry analyses combined with evolved gas analysis and pyrolysis-gas chromatography. In particular, py-GC/MS analyses were carried out in the double shot mode, derivatizing the sample with TMAH in the pyrolysis step at the lowest temperature, and then pyrolyzing the residual sample at 600 °C. This allowed: 1) to distinguish the various types of binders, 2) to define precisely the nature of the primary components of the alkyd binders, 3) to differentiate between thermochemolysis products and the more stable polymeric component of the alkyd binders, 4) to detect marker compounds of organic pigments.

This research is a first step towards the development of an integrated analytical protocol, including non-invasive and micro-destructive techniques, aimed at long-term monitoring of the state of conservation of urban artworks.

Acknowledgements

The authors wish to warmly thank Miss. Laura D'Amico for the contribution given during her master's degree thesis at the Department of Chemistry, University of Torino.
Funding: This work was supported by the European Commission, Programme Erasmus Plus, Key Action 2, Cooperation for innovation and the exchange of good practices - Knowledge Alliance 2017, Project N. 588082-EPP-A-2017-1-IT-EPPKA-KA.
The research was also part of the set-up of analytical procedures for the PRIN 2020 Project SuPerStAr - Sustainable Preservation Strategies for Street Art (2022-2025).

References

[1] P. Sanmartín, F. Cappitelli, Evaluation of Accelerated Ageing Tests for Metallic and Non-Metallic Graffiti Paints Applied to Stone, Coatings 7 (2017) 180. https://doi.org/10.3390/coatings7110180

[2] E.M. Alonso-Villar, T. Rivas, J.S. Pozo-Antonio, Resistance to artificial daylight of paints used in urban artworks. Influence of paint composition and substrate, Prog. in Org. Coat., 154 (2021) 106180. https://doi.org/10.1016/j.porgcoat.2021.106180

[3] P. Sanmartín, J.S. Pozo-Antonio, Weathering of graffiti spray paint on building stones exposed to different types of UV radiation, Constr. Build. Mater. 236 (2020) 117736. https://doi.org/10.1016/j.conbuildmat.2019.117736

[4] M.M. Di Crescenzo, E Zendri, M. Sánchez-Pons, L. Fuster-López, D.J. Yusá-Marco, The use of waterborne paints in contemporary murals: Comparing the stability of vinyl, acrylic and styrene-acrylic formulations to outdoor weathering conditions. Polym. Degrad. Stab. 107 (2014) 285–293. https://doi.org/10.1016/j.polymdegradstab.2013.12.034

[5] M. Baglioni, G. Poggi, Y.J. Benavides, F. Martínez Camacho, R. Giorgi, P. Baglioni, Nanostructured fluids for the removal of graffiti – A survey on 17 commercial spray-can paints, J. Cult. Herit., 34 (2018) 218-226. https://doi.org/10.1016/j.culher.2018.04.016

[6] A. Botteon, C. Colombo, M. Realini, S. Bracci, D. Magrini, P. Matousek, C. Conti, Exploring street art paitings by microspacially offset Raman spectroscopy, J. Raman Spectrosc. 49 (2018) 1652–1659. https://doi.org/10.1002/jrs.5445

[7] A. Macchia, S.A. Ruffolo, L. Rivaroli, M. Malagodi, M. Licchelli, N. Rovella, L. Randazzo, M.F. La Russa, Comparative study of protective coatings for the conservation of Urban Art, J. Cult. Herit. 41 (2020) 232-237. https://doi.org/10.1016/j.culher.2019.05.001

[8] C. Giusti, M. P. Colombini, A. Lluveras-Tenorio, J. La Nasa, J. Striova, B. Salvadori, Graphic vandalism: Multi-analytical evaluation of laser and chemical methods for the removal of spray paints, J. Cult. Herit., 44 (2020) 260-274. https://doi.org/10.1016/j.culher.2020.01.007

[9] M. Bertasa, C. Ricci, A. Scarcella, F. Zenucchini, G. Pellis, P. Croveri, D. Scalarone, Overcoming challenges in street art murals conservation: a comparative study on cleaning approach and methodology, Coatings 10 (2020) 1019. doi:10.3390/coatings10111019.
[10] J. La Nasa, S. Orsini, I. Degano, A. Rava, F. Modugno, M.P. Colombini, A chemical study of organic materials in three murals by Keith Haring: a comparison of painting techniques, Microchem. J., 124 (2016) 940-948. https://doi.org/10.1016/j.microc.2015.06.003
[11] G. Geminario, I.D. Van Der Werf, L. Sabbatini, Chemical characterization of spray paints by a multi-analythical (Py-GC/MS, FTIR, uRaman) approach, Microchem. J. 124 (2016) 929-939. https://doi.org/10.1016/j.microc.2015.04.016
[12] A. Bosi, A. Ciccola, I. Serafini, M. Guiso, F. Ripanti, P. Postorino, R. Curini, A. Bianco, Street art graffiti: Discovering their composition and alteration by FTIR and micro-Raman spectroscopy. Spectrochim. Acta - Part A Mol. Biomol. Spectrosc. 225 (2020) 117474. https://doi.org/10.1016/j.saa.2019.117474
[13] J. La Nasa, B. Campanella, F. Sabatini, A. Rava, W. Shank, P.Lucero-Gomez, D. De Luca, S. Legnaioli, V. Palleschi, M. P Colombini, I. Degano, F. Modugno, 60 years of street art: A comparative study of the artists' materials through spectroscopic and mass spectrometric approaches, J. Cult. Herit. 48, (2021) 129-140. https://doi.org/10.1016/j.culher.2020.11.016
[14] E. Jablonski, T. Learner, J. Hayes, M. Golden, Conservation concerns for acrylic emulsion paints, Stud. Conserv. 48 (2003) 3–12. https://doi.org/10.1179/sic.2003.48.Supplement-1.3
[15] N. Grassie, G. Scott, Polymer Degradation and Stabilisation, Cambridge University Press, Cambridge, 1985.
[16] M. Anghelone, D. Jembrih-Simbürger, V. Pintus, M. Schreiner. Photostability and influence of phthalocyanine pigments on the photodegradation of acrylic paints under accelerated solar radiation, Polym. Degrad. Stab. 146 (2017) 13–23. https://doi.org/10.1016/j.polymdegradstab.2017.09.013
[17] R. Ploeger, D. Scalarone, O. Chiantore, Thermal analytical study of the oxidative stability of artists' alkyd paints, Polym. Degrad. Stab. 94 (2009) 2036–2041. https://doi.org/10.1016/j.polymdegradstab.2009.07.018
[18] J. La Nasa, I. Degano, F. Modugno, M.P. Colombini, Effects of acetic acid vapour on the ageing of alkyd paint layers: Multi-analytical approach for the evaluation of the degradation processes, Polym. Degrad. Stab. 105 (2014) 257–264. https://doi.org/10.1016/j.polymdegradstab.2014.04.010

[19] V. Pintus, S. Wei, M. Schreiner, Accelerated UV ageing studies of acrylic, alkyd, and polyvinyl acetate paints: Influence of inorganic pigments, Microchem. J. 124 (2016) 949–961. https://doi.org/10.1016/j.microc.2015.07.009
[20] CAPuS, Conservation of Art in Public Spaces project. Work Package 3: Final Report. http://www.capusproject.eu/2020/03/31/work-package-3-final-report/, 2020 (accessed 12 March 2022).
[21] CAPuS, Conservation of Art in Public Spaces project. Glossary. http://www.capusproject.eu/glossary/, 2020 (accessed 12 March 2022).
[22] Witzel R. F., Burnham R. W., Onley J. W., Threshold and suprathreshold perceptual colour differences, J Opt Soc Am, 63(5), (1973) 615-625. https://doi.org/10.1364/JOSA.63.000615
[23] R. Ploeger, D. Scalarone, O. Chiantore, The characterization of commercial artists' alkyd paints, J. Cult. Herit. 9, (2008) 412–419. https://doi.org/10.1016/j.culher.2008.01.007
[24] P.K.T. Oldring, G. Hayward, A manual for resins for surface coatings, second ed., vol. 1. SITA Technology, London, 1987.
[25] H. Standeven, The development of decorative gloss paints in Britain and the United States c. 1910-1960, J. Am. Inst. Conserv. 45 (2006) 55-65. https://doi.org/10.1179/019713606806082210
[26] R. Van Gorkum, E. Bouwman, The oxidative drying of alkyd paints catalysed by metal complexes. Coord. Chem. Rev. 249 (2005) 1709–28. https://doi.org/10.1016/j.ccr.2005.02.002
[27] N. Sonoda, Characterization of Organic Azo-Pigments by Pyrolysis-Gas Chromatography, Stud. in Conserv. 44 (1999) 195-208. https://doi-org.bibliopass.unito.it/10.2307/1506705
[28] E. Ghelardi, I. Degano, M.P. Colombini, J. Mazurek, M. Schilling, T. Learner, Py-GC/MS applied to the analysis of synthetic organic pigments: characterization and identification in paint samples, Anal. Bioanal. Chem. 407 (2015) 1415–1431. https://doi-org.bibliopass.unito.it/10.1007/s00216-014-8370-y
[29] T. Fardi, V. Pintus, E. Kampasakali, E. Pavlidou, M. Schreiner, G. Kyriacou, Analytical characterization of artist's paint systems based on emulsion polymers and synthetic organic pigments, J. Anal. Appl. Pyrolysis, 135 (2018) 231-241. https://doi.org/10.1016/j.jaap.2018.09.001.

Figure captions

Figure 1. Colour change of the spray alkyd paints Montana94, Montana Gold and Belton Molotow after artificial ageing consisting of alternating cycles of exposure to artificial solar light and wet-dry cycles (as described in the Experimental section). The orange thick line represents the value beyond which the colour difference is objectively visible to the human eye.

Figure 2. Photographic documentation of the mock-ups under diffuse visible light (top) and UV radiation (bottom); for each set, the left column shows the mock-ups before ageing, while the right column after ageing - (a) Belton Molotow spray paint; (b) Montana Gold spray paint; (c) Montana94 spray paint.

Figure 3. FTIR spectra of unged and aged red alkyd spray paints: Belton Molotow (top), Montana Gold (centre), Montana94 (bottom).

Figure 4. SEM images at 800x magnifications showing the thickness of Montana94 black paint in the unaged (left) and aged (right) mock-ups.

Figure 5. EGA-MS curve of unaged and aged Belton Molotow alkyd spray paints.

Figure 6. Double-shot py-GC/MS of the three brands of black alkyd spray paints: T_{py}=240 °C (left), T_{py}=600 °C (right).

Figure 7. Reaction scheme of bis(2-ethylhexyl) adipate under thermally assisted hydrolysis and methylation.

Figure 8. *No title*, by Rojo Roma (2012), Turin, Italy. Photo credits: CAPuS project, 2018. Image of the mural (A) and details of the cracking and flaking of the paint film (B, C).

Figure 9. Pyrolysis-GC/MS analysis of a degraded paint sampled from the mural *No title*, by Rojo Roma (2012), Turin, Italy.

Table 1. List of the spray paints investigated.

Brand	Manufacturer	Classification	Colors
Montana94	Montana Colors	Alkyd	Red Green Black
Montana Gold	Montana-Cans	Alkyd-nitro-acrylic	Red Green Black
Belton Molotow Premium	Molotow	Alkyd-nitrocellulose	Red Green Black

Table 2. Colour measurements of the investigated spray paints.

	ΔL*	Δa*	Δb*	ΔE^*_{ab}
Montana94 Red	2.26±0.63	-1.56±1.43	-0.36±0.10	2.77±1.56
Montana94 Black	0.01±0.14	-0.04±0.03	-0.02±0.07	0.05±0.16
Montana94 Green	0.12±0.04	-0.18±0.03	-1.24±0.33	1.26±0.34
Montana Gold Red	-0.58±0.14	-1.38±1.08	-1.70±1.46	2.26±1.82
Montana Gold Black	-0.25±0.44	-0.02±0.00	0.12±0.05	0.28±0.45
Montana Gold Green	-1.03±0.54	-0.43±0.05	-0.69±0.36	1.32±0.65
Molotow Belton Red	1.57±0.85	-1.73±1.58	-1.93±0.92	3.03±2.03
Molotow Belton Black	2.26±0.99	-0.16±0.01	-0.63±0.08	2.35±0.99
Molotow Belton Green	1.96±0.45	-0.29±0.02	-0.07±0.01	1.98±0.45

Table 3. Pyrolysis products of the unaged alkyd spray paints identified. M94=Montana94, MG=Montana Gold, BM=Belton Molotow.

			First shot, T_{Py}=240 °C									Second shot, T_{Py}=600 °C								
Peak No.	Assignment	Retention time [min]	M94 black	M94 red	M94 green	MG black	MG red	MG green	BM black	BM red	BM green	M94 black	M94 red	M94 green	MG black	MG red	MG green	BM black	BM red	BM green
1	1,3-dimethoxy-2,2-dimethyl-propane	2.9				X	X	X	X	X	X									
2	1,2,3-trimethoxy propane	4.7	X	X	X	X	X	X	X	X	X									
3	Styrene	4.8													X	X	X			
4	Methoxymethyl benzene	6.3							X	X	X									
5	2-ethyl-1-hexanol	7.1				X	X	X												
6	1,3-dimethoxy-2-(methoxymethyl)-2-methyl-propane	7.7							X	X	X*									
7	Unidentified carboxylic acid methyl ester	7.9				X	X	X	X	X	X				X	X	X	X	X	X
8	Benzoic acid methyl ester	8.3	X	X	X							X	X	X	X	X	X	X	X	X
9	1,3-dimethoxy-2,2-bis(methoxymethyl)-propane	8.8	X	X	X	X	X	X	X	X	X									
a	N-methyl-o-toluidine	9.3					X									X				
b	1,2,4-trichloro-benzene	9.6					X									X				
c	2-methoxy-benzenamine	9.6		X				X												
10	3-methoxy-2,2-bis(methoxymethyl)-1-propanol	9.8	X	X	X	X	X	X	X	X	X				X*	X*	X*			
11	Hexanedioic acid dimethyl ester, dimethyl adipate	10.5				X	X	X							X	X	X			
d	2-ethoxy-benzenamine	10.6								X										
e	N-methyl-2-methoxy-benzenamine	10.7		X				X												

f	3-chloro-N-methyl-benzenamine	11.2								X									X	
12	Phthalic anhydride	11.7										X	X	X	X	X	X			
g	1,2-benzendicarbonitrile	12.0												X			X			
h	4-cyano-benzoic acid methyl ester	12.9												X			X			X
13	1,2-benzendicarboxylic acid dimethyl ester (dimethyl phthalate)	13.5	X	X	X	X	X	X	X	X	X	X	X	X	X	X	X	X	X	X
14	Nonandioic acid dimethyl ester (azelaic acid dimethyl ester)	14.5	X	X	X							X	X	X						
i	2,4,5-trichloro-benzenamine	14.6					X									X				
15	1-hexadecene	15.0	X	X	X	X	X	X	X	X	X									
16	Tetradecanoic acid methyl ester	16.5	X	X	X				X		X									
17	1-octadecene	17.2	X	X	X	X			X	X	X									
18	N,N-dimethyl-hexadecanamine	18.4	X	X	X	X	X	X	X	X	X									
19	Hexadecanoic acid methyl ester (pamitic acid methyl ester)	18.6	X	X	X	X*	X*	X*	X	X	X	X*	X*	X*	X*	X*		X*	X*	X
20	9-octadecenoic acid methyl ester (oleic acid methyl ester)	20.3	X	X	X				X	X	X	X*	X*	X*				X*	X*	X*
21	Octadecanoic acid methyl ester (stearic acid methyl ester)	20.6	X	X	X	X*	X*	X*	X	X	X	X*	X*	X*				X*	X*	X
22	9,12-octadecadienoic acid methyl ester (linoleic acid methyl ester)	20.7	X	X	X				X	X	X									
23	9,12-octadecadienoic acid methyl ester, isomer	20.8							X	X										

24	9,12-octadecadienoic acid methyl ester, isomer	21.1	X	X	X				X	X	X								
25	Eicosanoic acid methyl ester	22.3	X	X	X														
26	Dihydroxy-octadecanoic acid methyl ester**	22.5	X	X	X														
27	Bis(2-ethylhexyl) adipate	22.9				X	X	X											

*low intensity compared to the intensity of the same peak in other samples

**tentative assignment

Table 4. Pyrolysis products of the aged alkyd spray paints identified. M94=Montana94, MG=Montana Gold, BM=Belton Molotow.

			First shot, T_{Py}=240 °C									Second shot, T_{Py}=600 °C								
Peak No.	Assignment	Retention time [min]	M94 black	M94 red	M94 green	MG black	MG red	MG green	BM black	BM red	BM green	M94 black	M94 red	M94 green	MG black	MG red	MG green	BM black	BM red	BM green
1	1,3-dimethoxy-2,2-dimethyl-propane	2.9																		
2	1,2,3-trimethoxy propane	4.7	X	X	X	X	X	X	X		X									
3	Styrene	4.8													X	X	X			
4	Methoxymethyl benzene	6.3							X	X	X									
5	2-ethyl-1-hexanol	7.1				X*	X*	X												
6	1,3-dimethoxy-2-(methoxymethyl)-2-methyl-propane	7.7							X	X	X									
7	Unidentified carboxylic acid methyl ester	7.9				X	X	X	X	X	X				X	X	X	X	X	X
8	Benzoic acid methyl ester	8.3	X	X	X							X	X	X	X	X	X	X	X	X
9	1,3-dimethoxy-2,2-bis(methoxymethyl)-propane	8.8	X	X	X	X	X	X	X	X	X									
a	N-methyl-o-toluidine	9.3					X									X				
b	1,2,4-trichloro-benzene	9.6																		
c	2-methoxy-benzenamine	9.6		X				X												
10	3-methoxy-2,2-bis(methoxymethyl)-1-propanol	9.8	X	X	X	X	X	X	X	X	X				X*	X*	X*			
11	Hexanedioic acid dimethyl ester, dimethyl adipate	10.5																		
d	2-ethoxy-benzenamine	10.6								X										
e	N-methyl-2-methoxy-benzenamine	10.7		X				X												

f	3-chloro-N-methyl-benzenamine	11.2								X									
12	Phthalic anhydride	11.7											X	X					
g	1,2-benzendicarbonitrile	12.0												X			X		
h	4-cyano-benzoic acid methyl ester	12.9												X			X		X
13	1,2-benzendicarboxylic acid dimethyl ester (dimethyl phthalate)	13.5	X	X	X	X*	X*	X	X	X	X	X	X	X	X	X	X	X	X	X
14	Nonandioic acid dimethyl ester (azelaic acid dimethyl ester)	14.5	X	X	X				X	X	X	X	X	X				X	X	X
i	2,4,5-trichloro-benzenamine	14.6					X									X				
15	1-hexadecene	15.0							X	X	X									
16	Tetradecanoic acid methyl ester	16.5	X						X	X	X									
17	1-octadecene	17.2	X						X	X	X									
18	N,N-dimethyl-hexadecanamine	18.4	X			X	X	X	X											
19	Hexadecanoic acid methyl ester (pamitic acid methyl ester)	18.6	X	X	X	X*	X*	X	X	X	X	X*	X*	X*			X	X	X*	X*
20	9-octadecenoic acid methyl ester (oleic acid methyl ester)	20.3	X	X*	X							X*		X*						
21	Octadecanoic acid methyl ester (stearic acid methyl ester)	20.6	X	X	X		X*	X	X	X	X	X*	X*	X*			X	X	X*	X*
22	9,12-octadecadienoic acid methyl ester (linoleic acid methyl ester)	20.7																		
23	9,12-octadecadienoic acid methyl ester, isomer	20.8																		

24	9,12-octadecadienoic acid methyl ester, isomer	21.1			X*														
25	Eicosanoic acid methyl ester	22.3	X	X															
26	Dihydroxy-octadecanoic acid methyl ester**	22.5	X	X								X*	X*	X*					
27	Bis(2-ethylhexyl) adipate	22.9																	

*low intensity compared to the intensity of the same peak in other samples

**tentative assignment

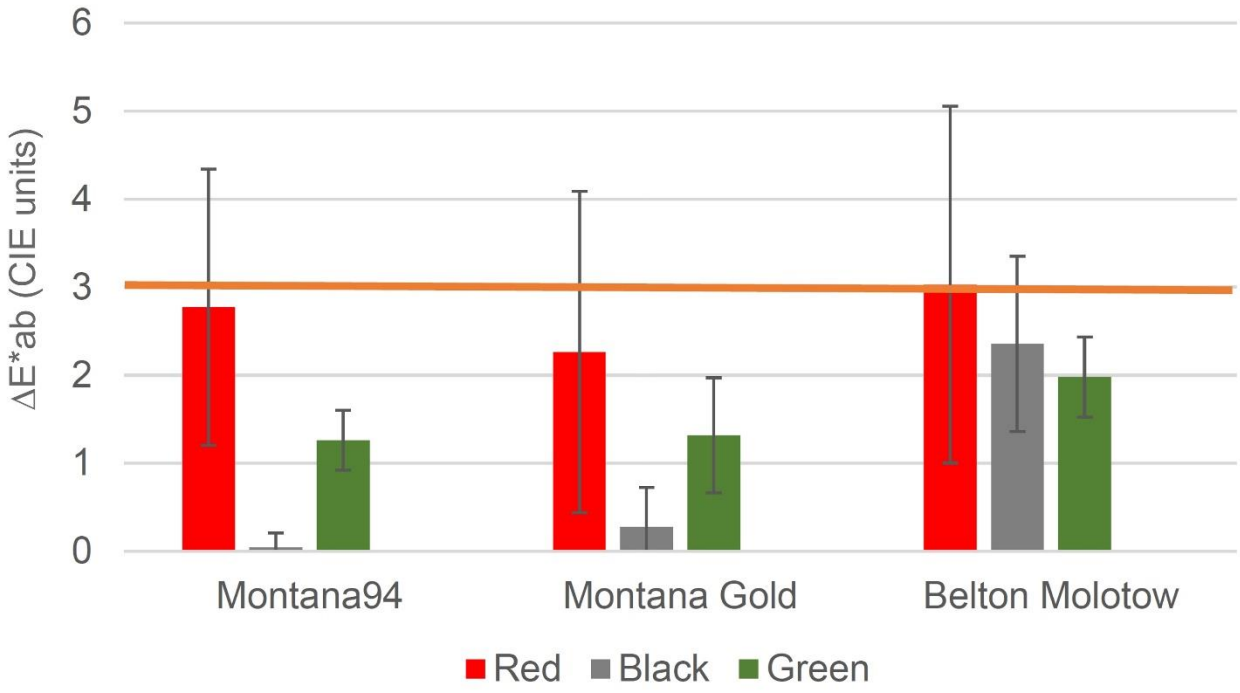

Figure 1. Colour change of the spray alkyd paints Montana94, Montana Gold and Belton Molotow after artificial ageing consisting of alternating cycles of exposure to artificial solar light and wet-dry cycles (as described in the Experimental section). The orange thick line represents the value beyond which the colour difference is objectively visible to the human eye.

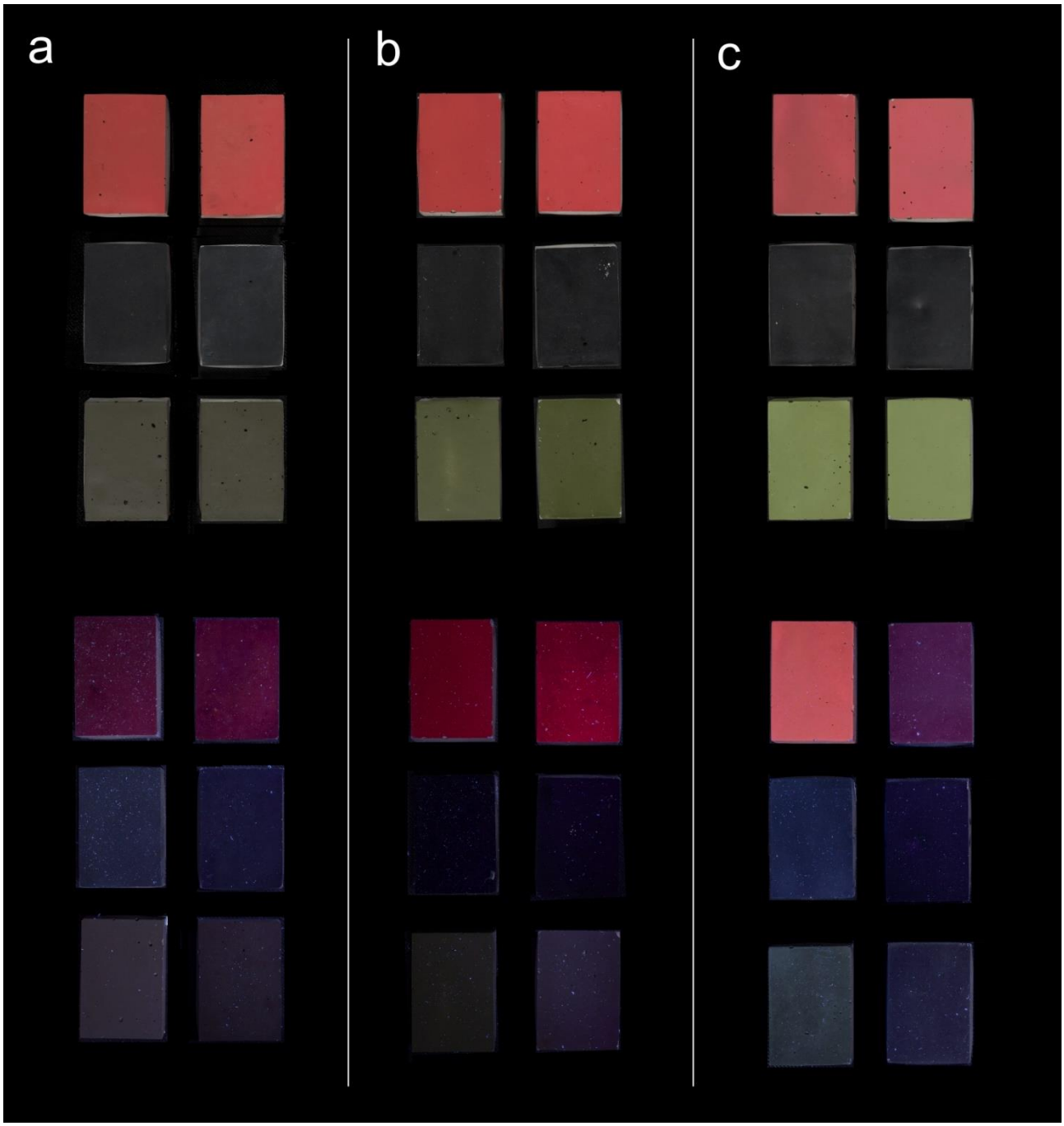

Figure 2. Photographic documentation of the mock-ups under diffuse visible light (top) and UV radiation (bottom); for each set, the left column shows the mock-ups before ageing, while the right column after ageing - (a) Belton Molotow spray paint; (b) Montana Gold spray paint; (c) Montana94 spray paint.

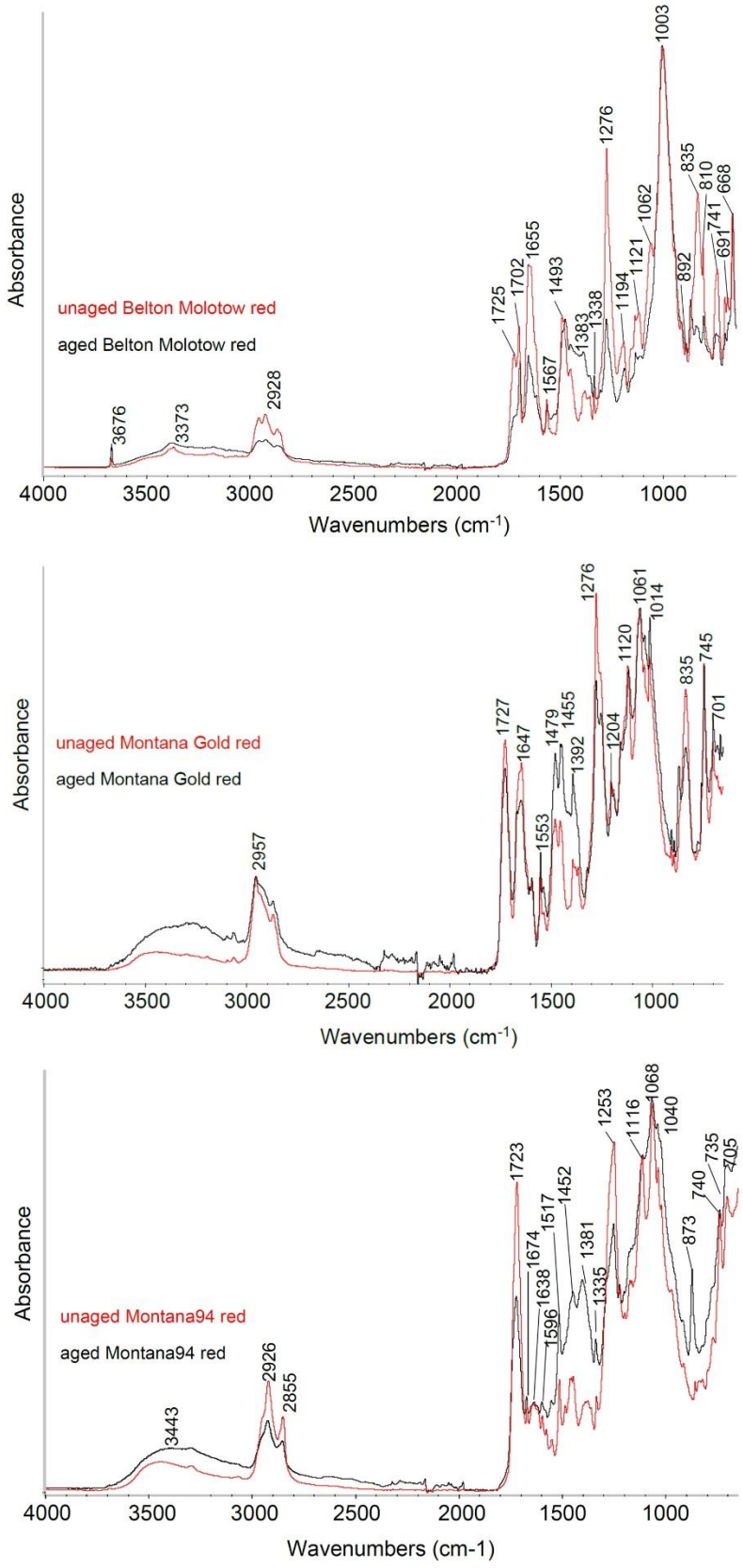

Figure 3. FTIR spectra of unged and aged red alkyd spray paints: Belton Molotow (top), Montana Gold (centre), Montana94 (bottom).

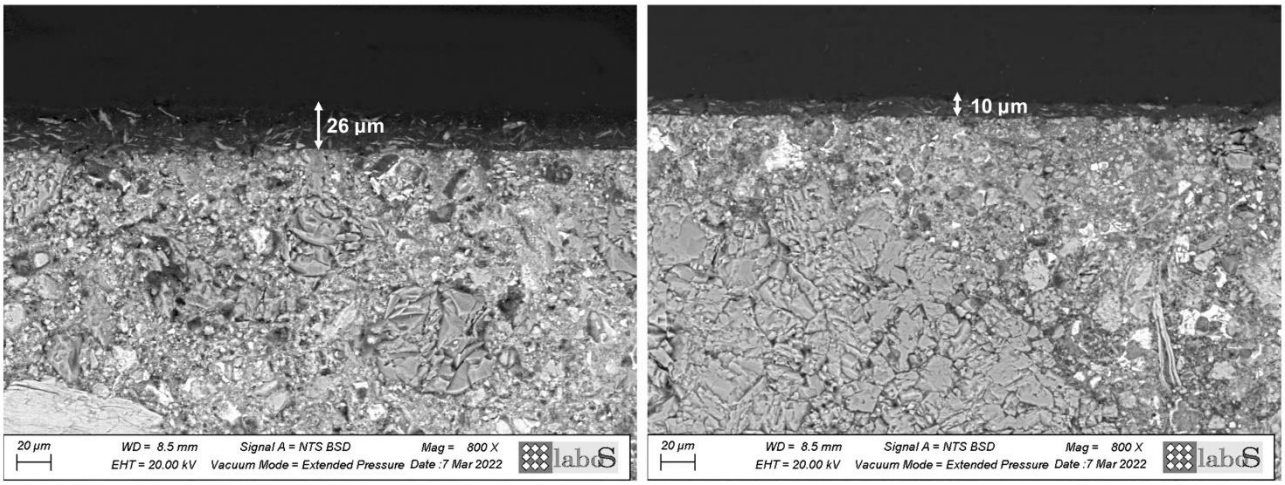

Figure 4. SEM images at 800x magnifications showing the thickness of Montana94 black paint in the unaged (left) and aged (right) mock-ups.

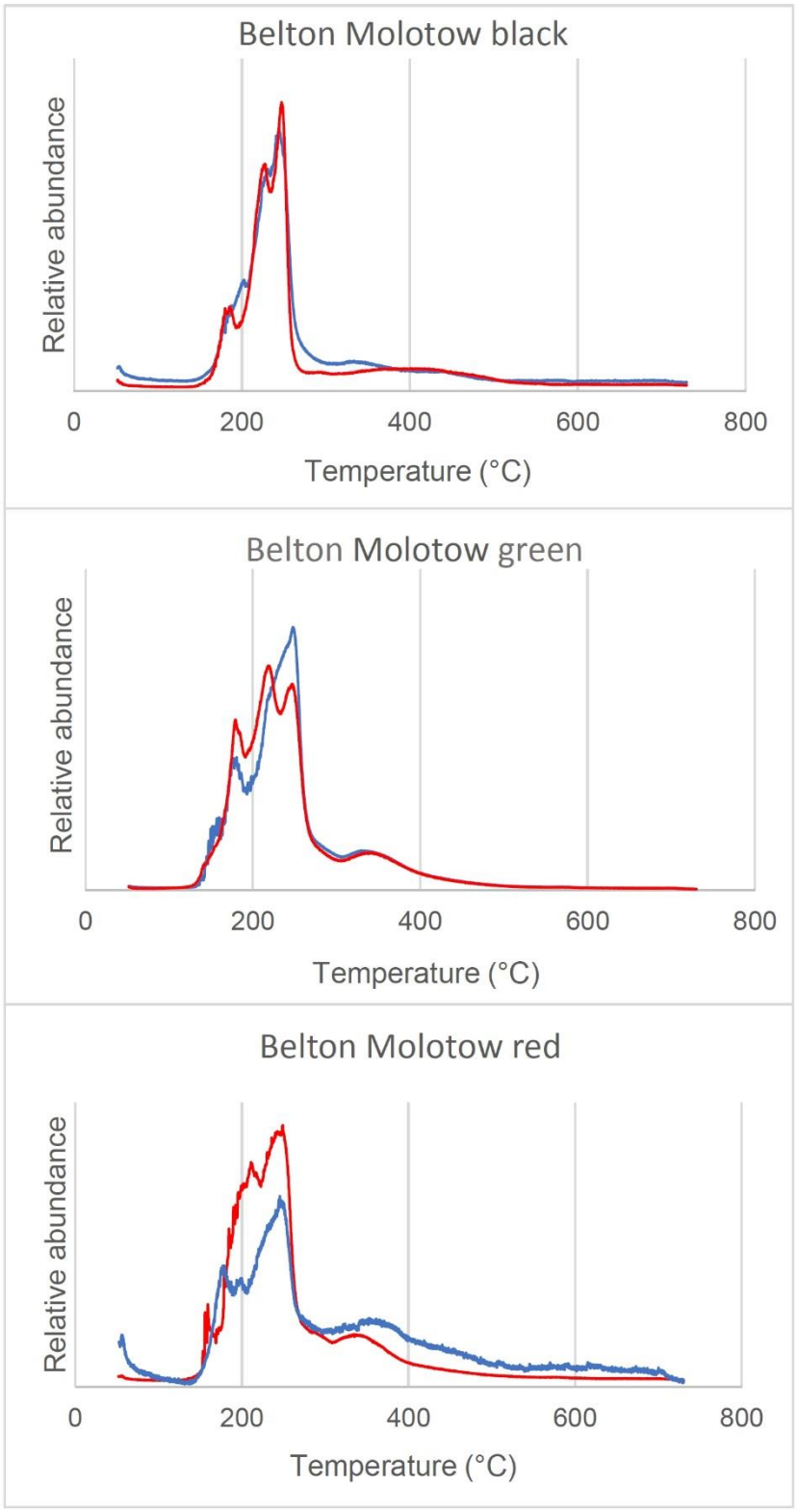

Figure 5. EGA-MS curve of unaged and aged Belton Molotow alkyd spray paints.

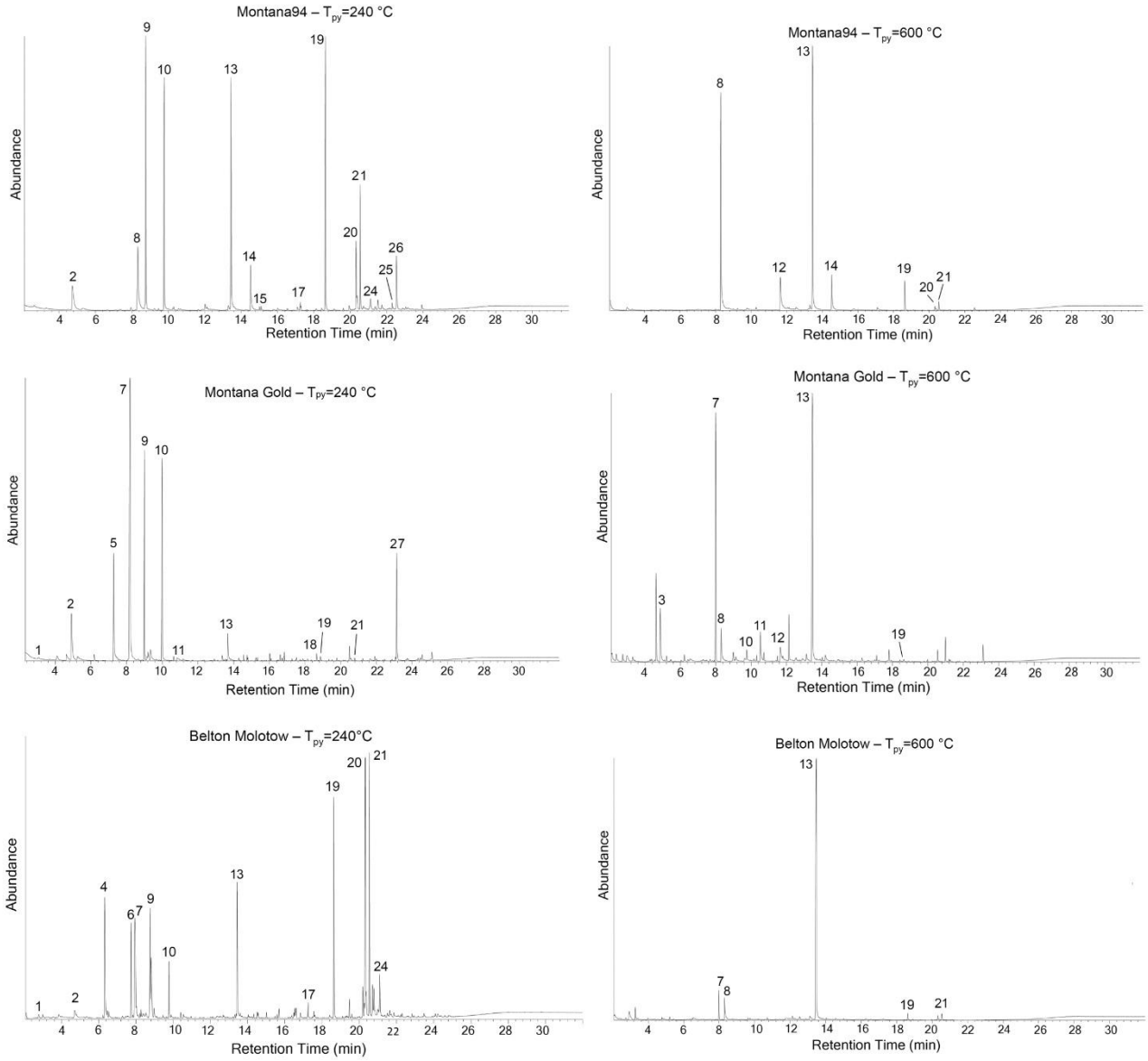

Figure 6. Double-shot py-GC/MS of the three brands of black alkyd spray paints: T_{py}=240 °C (left), T_{py}=600 °C (right).

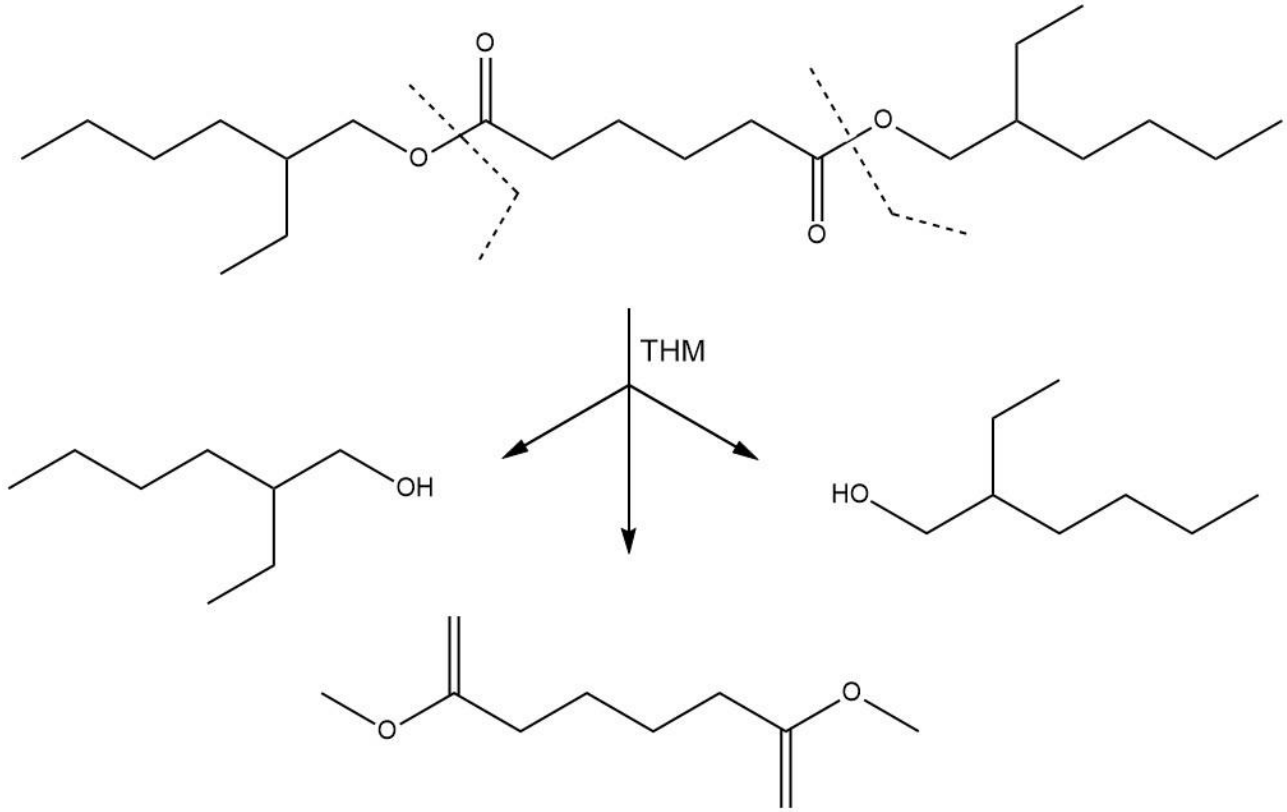

Figure 7. Reaction scheme of bis(2-ethylhexyl) adipate under thermally assisted hydrolysis and methylation.

Figure 8. *No title*, by Rojo Roma (2012), Turin, Italy. Photo credits: CAPuS project, 2018. Image of the mural (A) and details of the cracking and flaking of the paint film (B, C).

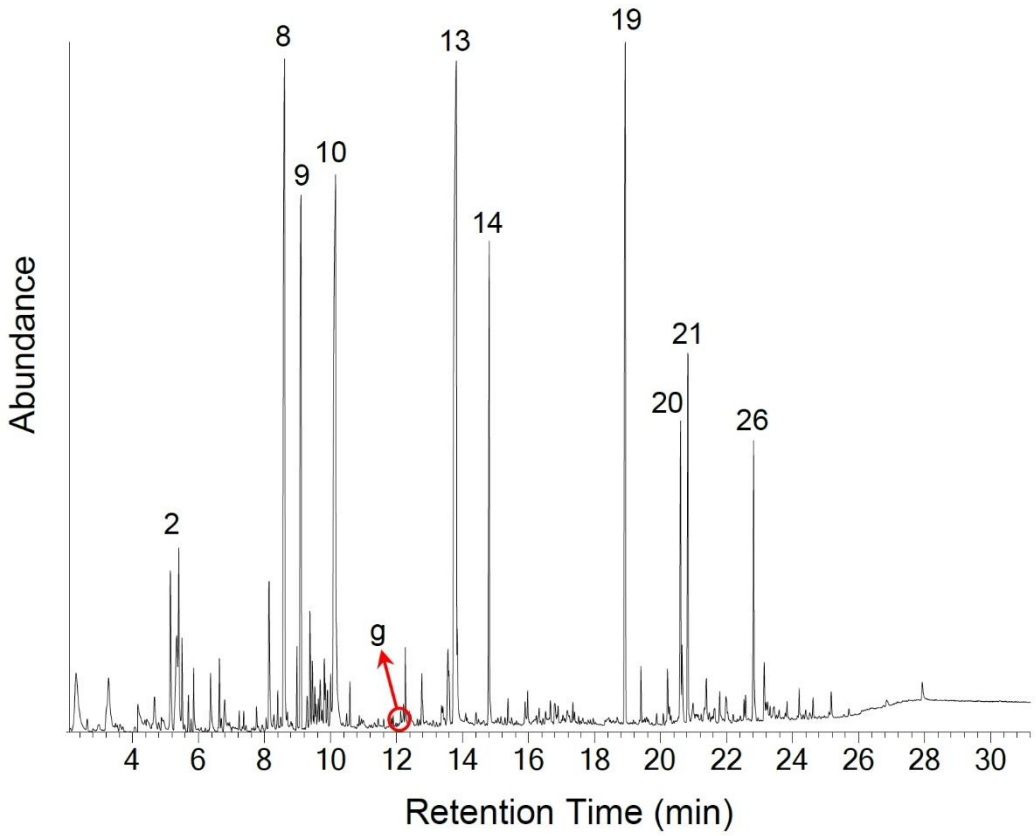

Figure 9. Pyrolysis-GC/MS analysis of a degraded paint sampled from the mural *No title*, by Rojo Roma (2012), Turin, Italy.